Journal of NanoScience, NanoEngineering & Applications
Volume 2, Issue 1, April 2012, Pages 23-37

Synthesis of Metallic Copper Nanoflowers, Nanocrystals and Nanorods using Electrodeposition and Hydrothermal Techniques

Hardev Singh Virk*
Professor Emeritus, Eternal University, Baru Sahib (HP), India

ABSTRACT

Copper nanoflowers and nanocrystals have been fabricated using two different techniques; electro-deposition of copper in polymer and anodic alumina templates (AAT) and Cetyltrimethyl-ammonium Bromide (CTAB)-assisted hydrothermal method. Nanorods of copper are produced by electrodeposition in 100 nm AAT. Scanning Electron Microscope (SEM) micrographs record some interesting morphologies of metallic copper nanoflowers and nanocrystals. Field Emission Scanning Electron Microscope (FESEM) has been used to determine morphology and chemical composition of polycrystalline copper oxide nanocrystals and nanorods. X-ray diffraction (XRD) pattern reveals the polycrystalline nature of copper nanocrystals and monoclinic phase of CuO in the crystallographic structure of copper oxide nanoflowers. The synthesis of nanoflowers and other exotic patterns is due to over-deposition in nanopores of templates which is explained by Erdey-Gruz and Volmer relationship between the over-potentials and the nucleation rates. There is no repeatability in the experiments for synthesis of micro/nano crystals and flowers, which proves that they belong to the realms of both art and science.

Keywords: *Electrodeposition, hydrothermal method, anodic alumina template, nanopores, nanoflowers, nanocrystals, nanorods, polycrystalline, nucleation rate*

****Author for Correspondence:*** E-mail: hardevsingh.virk@gmail.com; Tel. No. : 9417553347

1. INTRODUCTION

Copper is one of the most important metals in modern electronic technology. Keeping in view its role in nanoelectronics, we have fabricated copper nanowires of diameters 100 and 200 nm using anodic alumina and polymer membranes as templates. Template-based growth of copper nanowires has been realized using conventional electrodeposition technique in an electrochemical cell designed in our laboratory [1–4]. It was observed that in case of polymer templates, in general, and in anodic alumina templates (AAT), in particular, if the template was not coated with a conducting layer before electrodeposition, it resulted in failure to grow nanowires. But the failure of experiment proved to be a blessing in disguise. Instead of copper nanowires, we observed the growth of nanoflowers, polycrystalline copper crystals and other exotic patterns [4–6]. It is anticipated that copper ions from the electrolyte do not enter template pores due to poor conductivity but get deposited on the cathode surface in the form of polycrystalline crystals.

During the last decade, exhaustive reviews [7–10] have been published on metal nanostructures. A series of various nanoflowers and nanoflower-like structures have been obtained, depending on reaction conditions, such as reagents ratio, temperature and other conditions. Nanoflower structure

may consist of such more simple nanostructures, as nanorods, nanowalls, or nanowires. Current and possible applications of nanoflowers as optoelectronics devices or sensors, in catalysis, and solar cells caused a definite interest in them. Nanoflowers of almost all metals have been reported in the form of elemental nanoflowers; metal oxide nanoflowers; nanoflowers of hydroxides and oxosalts; sulphide, selenide, and telluride nanoflowers; nitride and phosphide nanoflowers; nanoflowers formed by organic and coordination compounds [7].

Flower-like cupric oxide (CuO) nanostructures have been prepared via Cetyltrimethyl-ammonium Bromide (CTAB)-assisted hydrothermal method [11]. CTAB is a useful surfactant that has been widely used in fabricating the nanomaterials to control the morphology. Cao et al. [12] reported CTAB-assisted hydrothermal synthesis of CuO of various morphologies such as rod-like, spheriodal, hexahedron, and other irregular structures. Author's group have reported fabrication and characterization of copper nanowires and some exotic patterns of polycrystalline copper recently using electrodeposition technique of template synthesis and CTAB-assisted hydrothermal method [1–6].

2. MATERIALS AND METHODS

There are several techniques for synthesis of nanoflowers as reported in various reviews [7–10]. We followed two different routes for preparation of copper nanoflowers and nanocrystals: electro-deposition technique using template synthesis and CTAB-assisted hydrothermal method.

Electro-deposition technique used in our experiment [1–4] is similar in principle to that used for the electroplating process. Commercially available polycarbonate membranes (Sterlitech, USA) of 25 mm diameter with pore density of 10^8 pores/cm^2 and pore diameter of 100 nm were selected for this experiment.

The main purpose of this experiment was to fabricate nanowires of copper. However, to our utter surprise, we failed in our mission and what we got was a blessing in disguise. We observed formation of some exotic patterns, including synthesis of nanoflowers. A second set of experiments was completed using commercial anodic alumina membranes (anodisc 25 made by Whatman) having pore diameters of 100 and 200 nm, a nominal thickness of 60 μm and a pore density of 10^9 pores/cm^2 as templates.

Electrodeposition was carried out in an electrochemical cell of cylindrical shape fabricated in our laboratory using Perspex sheets. A copper rod of 0.5 cm diameter and length equal to height of cylinder was used as an anode. The cathode consists of copper foil attached to polymer template by an adhesive tape of good conductivity. The electrolyte used

had a composition of 20 gm/100mL $CuSO_4 \cdot 5H_2O$ + 25% of dilute H_2SO_4 at room temperature. The inter-electrode distance was kept 0.7 cm and a current of 2 mA was applied for 10 min. The polymer template was dissolved in dichloromethane to liberate copper nanoflowers from the host matrix.

Copper nanowires can be produced generally using AAT with silver or copper thin layer thermally evaporated on one side to make it a good conductor. To produce exotic patterns, for example, polycrystalline nanocrystals and nanoflowers, we used AAT of 100 nm without coating its lower surface with copper or silver. The experimental conditions were also suitably modified to allow for overdeposition over the cathode surface.

A current of 40 mA was applied for 7 min, keeping other parameters the same as for polymer template electrodeposition. The grown nanostructures were liberated by dissolving alumina template in 1 M NaOH for 1 h in a beaker, washed in distilled water and dried in an oven at 50ºC for 30 min. The Scanning Electron Microscope (JEOL, JSM 6100) was used to record top and side views of grown nanostructures at an accelerating voltage of 20 kV using different magnifications.

For hydrothermal synthesis of CuO nanoflowers [11], analytical grade (Loba Chemicals) copper chloride dihydrate, $CuCl_2 \cdot 2H_2O$, and sodium hydroxide, NaOH, were used as precursors and CTAB as surfactant. All the chemicals were directly used without further purification and de-ionized water was used for preparation of solution.In a typical synthesis, the copper chloride solution was prepared by dissolving 0.8524 g (5 mmol) of $CuCl_2 \cdot 2H_2O$ in 20 mL de-ionized water. Subsequently, the copper chloride solution was slowly dropped into 50 mL of NaOH solution (3 mol L^{-1}) under vigorous stirring.

The blue-colored precursor was obtained. One gram of CTAB (3 mmol) was added to the blue-colored precursor and stirred vigorously for 30 min at 50 ºC to ensure the complete dissolution of CTAB. This reaction solution was then transferred to a 50 mL Teflon-lined stainless steel autoclave and heated at 150 º C for 12 h in an electric oven. After reaction, autoclave was allowed to cool to room temperature. The resulting black precipitate was centrifuged and washed thoroughly with de-ionized water and ethanol. Then the precipitate was dried in drying oven at 50 ºC for 24 h. Finally, the reaction products were calcined in a furnace at 500 ºC for 2h in an ambient air atmosphere.

X-ray Diffraction studies were carried out at Sophisticated Analytical Instruments Facility (SAIF) set up by Punjab University, Chandigarh using X'Pert PRO (PANanalytical, Netherlands) using Cu Kα radiation. Field Emission Scanning Electron Microscope (FESEM, Hitachi S-4300) was used to

determine chemical composition and energy dispersive X-ray (EDX) spectrum of grown nanorods and CuO nanoflowers.

3. RESULTS AND DISCUSSION

There is as yet no specific theory to explain exotic patterns developed during electro-deposition of copper in anodic alumina or polymer templates. A speculative explanation [13] is provided on the basis of over-deposition. The exotic patterns in the form of micro-flowers having their petals in nanometer dimension, copper buds leading to mushroom effect and double pyramid-shaped copper crystals have been observed in our investigations [4–6]. Flower-like morphology of metal over-deposits has been attributed to the changes in hydrodynamic conditions due to excessive hydrogen evolution during electro-deposition process [14].

During our recent experiments, we observed that the growth of nanoflowers depends upon two factors: cathode over- potential and conductivity of the cathode surface. If the conducting film is used for the cathode surface, Cu ions will tend to deposit into nanochannels of polymer template, otherwise they tend to grow laterally on the cathode surface. The deposition of copper takes place only when the potential of the cathode is lower than the equilibrium electrode potential of the electrolytic cell; hence, a certain magnitude of cathode over-potential is necessary. The relationship between the over-potentials and the nucleation rates was given by Erdey-Gruz and Volmer [15] as follows:

$$N = a\, e^{-b/\eta k2} \quad (1)$$

where N is the nucleation rate; η_k is the cathode over-potential; a and b are constants. It can be seen that the higher the over-potential, the higher the nucleation rates of growth. At a certain optimum over-potential, nanoflower fabrication occurs.

SEM micrographs of copper nanoflowers synthesis using polymer templates are shown in Figures 1 and 2. Figure 1 shows the deposition of copper in the form of flower petals. These flower petals, also called nanoflakes [16], are believed to have resulted from a nucleation process governed by an aggregation-mediated crystallization. Figure 2 depicts a garden of copper nanoflowers of identical shape where nanoflakes emerge from a nucleus to form petals of nanodimensions. The beauty of these experiments is that no identical patterns are produced on repeating the experiment. It remains an enigma and defies scientific explanation.

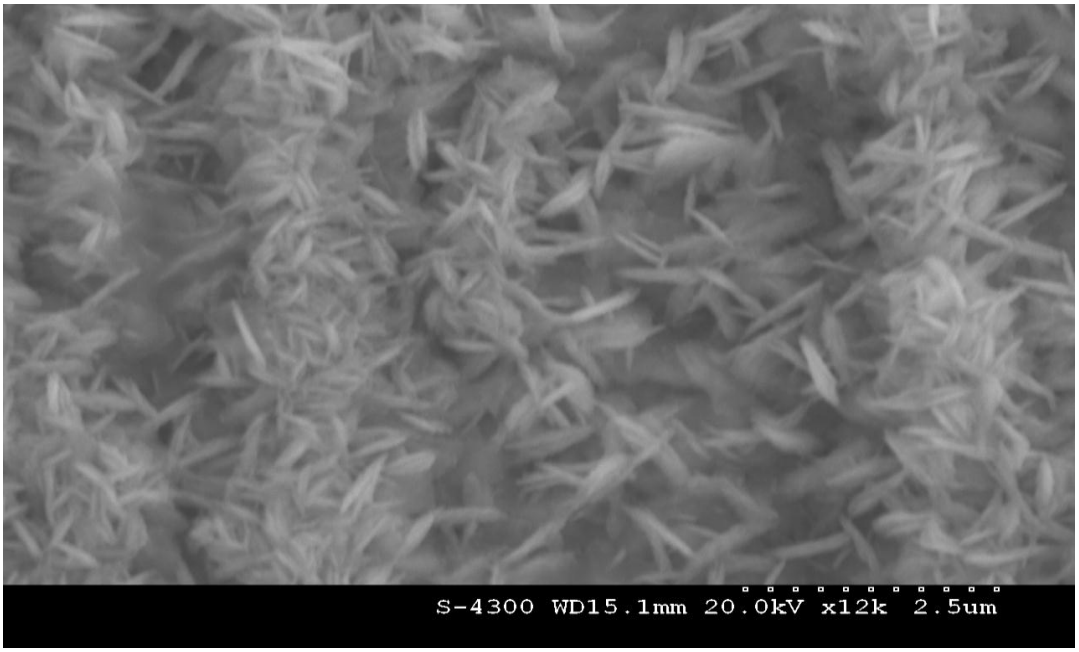

Fig.1: *SEM Micrograph of Copper Nanoflower Petals Grown in Polymer Template of 100 nm Pores.*

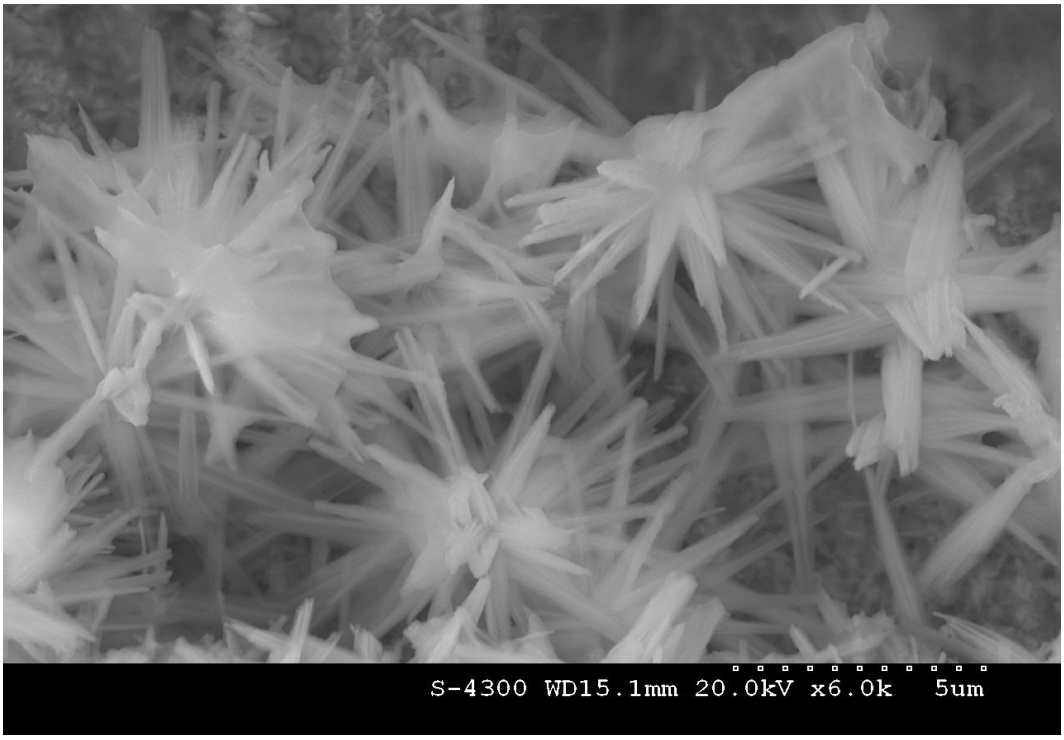

Fig. 2: *SEM Micrograph of Copper Nanoflowers Grown in Polymer Template of 100 nm Pores.*

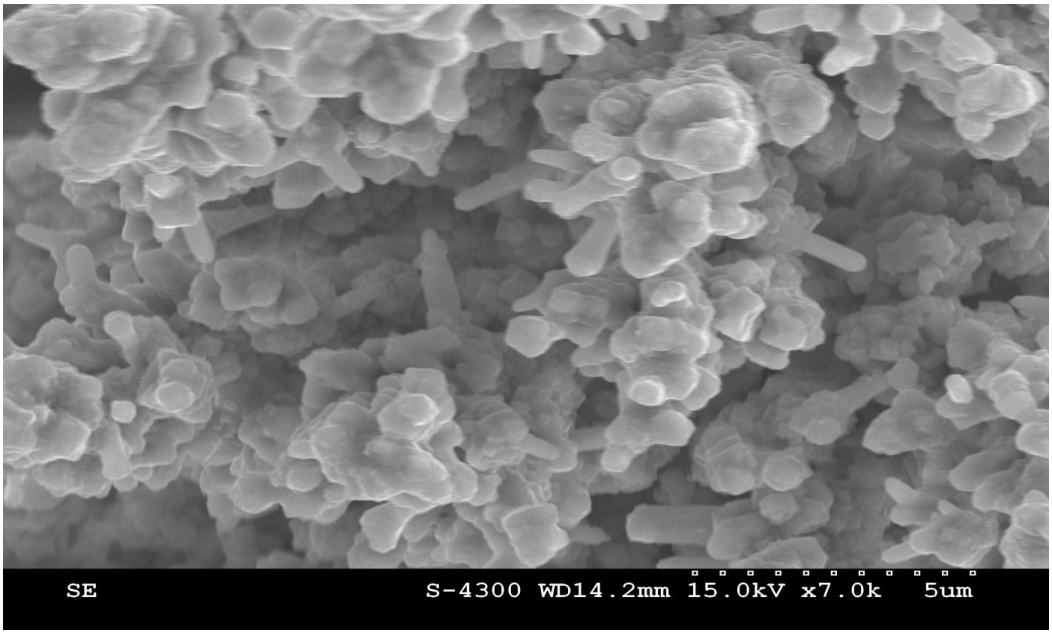

Fig. 3: *SEM Micrograph of Polycrystalline Cu Crystals Grown in AAT of 100nm Pore Diameter.*

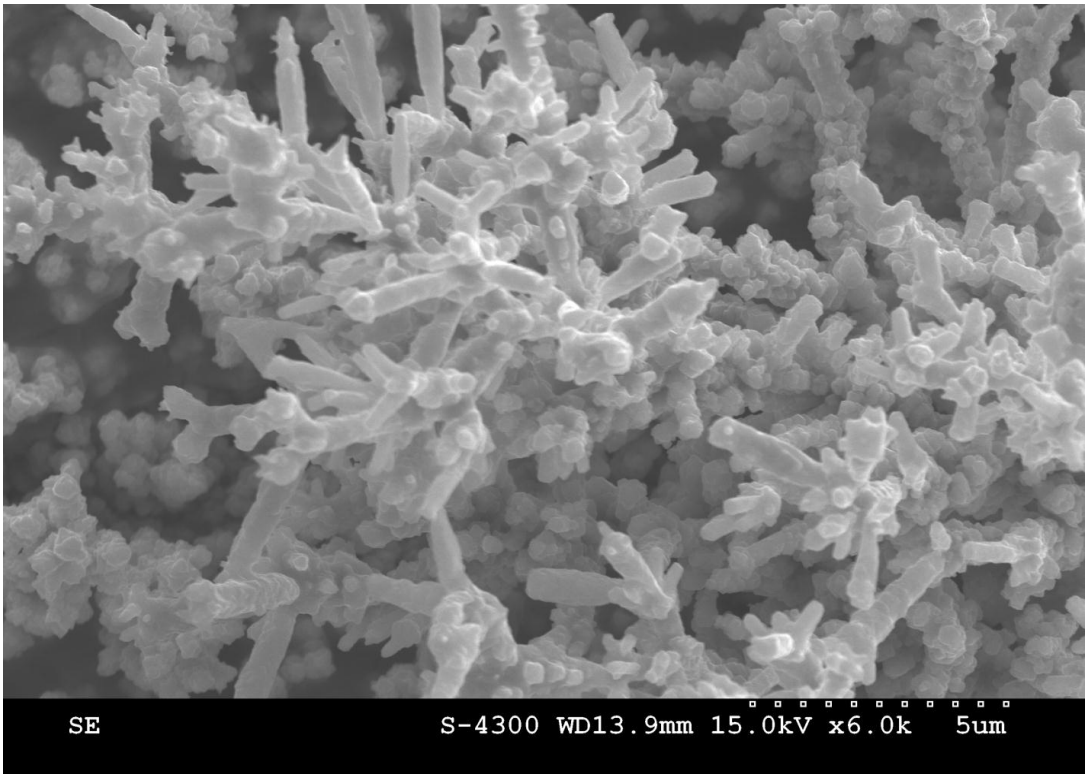

Fig. 4: *SEM Micrograph of Copper Nanoflowers Grown in AAT of 100 nm Pore Diameter.*

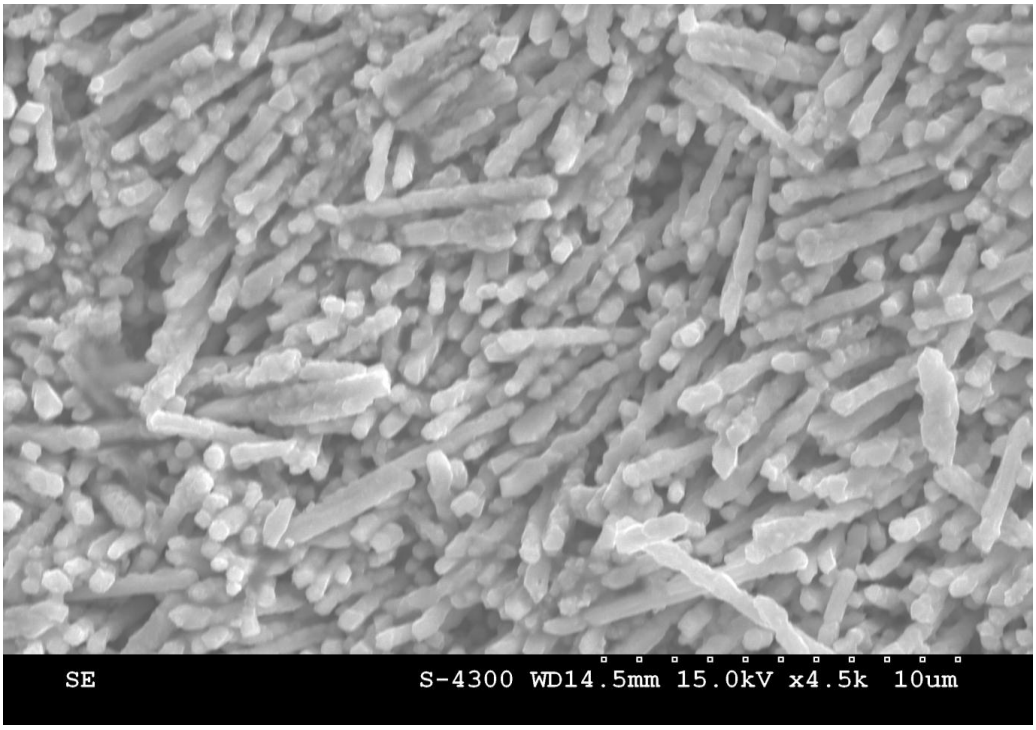

Fig. 5: *SEM Micrograph of Copper Nanorods Grown in AAT of 100 nm Pore Diameter.*

In the case of AAT, it was observed that if the template is not sputter coated with a conducting film, the copper nanowires were synthesised in the central region and nanoflowers in the peripheral zone [1]. It shows differential deposition of copper on the cathode surface. It is difficult to determine the exact conditions under which nanoflowers are synthesized along with nanowires. Our investigations reveal that chance plays a predominant role in growth of nanoflowers. The most disturbing feature of our study is that different types of nanostructures are created under similar experimental conditions. There is an element of random artistic design in nanoflowers fabricated in our laboratory. However, there is one satisfaction that all these exotic patterns find some analogue in nature. During the present series of experiments using AAT of 100 nm pore diameter, we used both sputter coated and as received templates. In case of unsputtered, or as received templates, we observed synthesis of polycrystalline copper crystals (Figure 3) and nanoflowers (Figure 4) grown on the cathode surface when alumina template was dissolved in 1 M NaOH for 1 h in a beaker under gentle shaking. These flower shapes have nothing in common with those of Figure 2, grown in polymer templates. Surprisingly, when the experiment was repeated using sputter coated alumina template of 100 nm pore dia. with a thin film of copper, the growth of nanorods of identical shape was observed in abundance (Figure 5).

To investigate the structure of copper nanocrystals and nanoflowers, XRD spectra

were recorded. XRD diffractograms were obtained in the 2θ range from 10º to 80º with a step of 0.02º, using the Cu K_α radiation source of λ=1.5406 Å. The crystal structure of these pentagon shaped copper crystals has been determined using X-ray diffraction analysis. XRD spectrum (Figure 6) shows two prominent peaks corresponding to 2θ = 43.4459 and a double peak around 2θ = 50.5912, with d spacing = 2.081 and 1.802, respectively (Table 1). These peaks reveal the polycrystalline nature of copper crystals, indicating that preferred growth direction of crystals is the (200) plane. The results are in exact agreement with the crystal structure of the pyramid shaped copper crystals already reported by the author [2].

XRD spectrum of copper nanoflowers (Figure 7) shows some interesting results. There are in all 10 peaks in the spectrum (Table II); with the most prominent peak at 2θ = 50.5565, and a triplet peak of considerable intensity around 2θ = 43.6140. There is a doublet peak at 2θ = 74.5117, but all other peaks are of negligible intensity and may be ignored. These peaks reveal the polycrystalline nature of copper nanoflowers, the most prominent peak at 2θ=50.5565, indicating that the preferred growth direction of nanoflowers is the (200) plane. On comparison of spectra of copper nanocrystals and nanoflowers, we come to the conclusion that the preferred growth direction is the same in both the cases. Synthesis of polycrystalline nanowires has been reported by the author [6] using electrodeposition in AAT.

The average crystallite size *D* of the Cu nanoflowers is calculated using the Debye Scherrer's formula [17]: $D = 0.9\ \lambda / \beta \cos \theta$, where λ=1.5406 Å is the wavelength of the X-ray radiation used, β is the full width at half maximum (FWHM) of the diffraction peak (0.1224), K, the shape factor is assumed to be 0.9 and θ is the Bragg diffraction angle of the most prominent XRD peak. Substituting appropriate values in the formula, the crystallite grain size value of Cu nanoflowers comes out to be 1.20 nm.

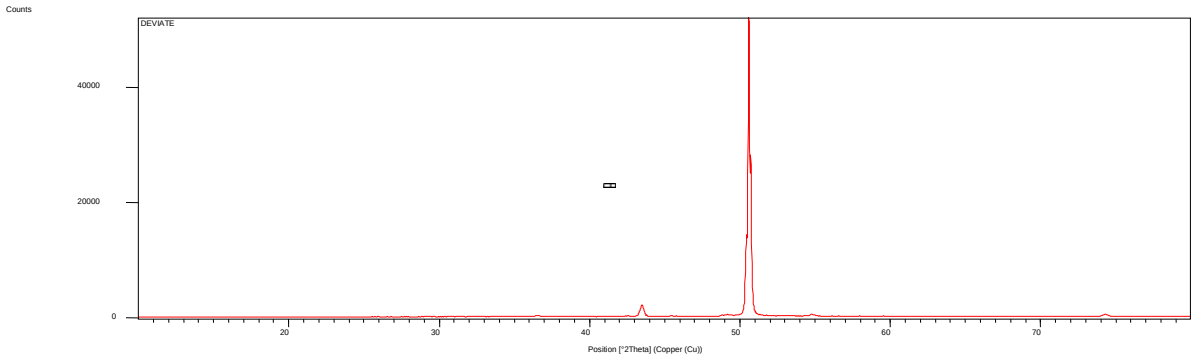

Fig. 6: *XRD Spectrum of Polycrystalline Pentagon-shaped Copper Crystals.*

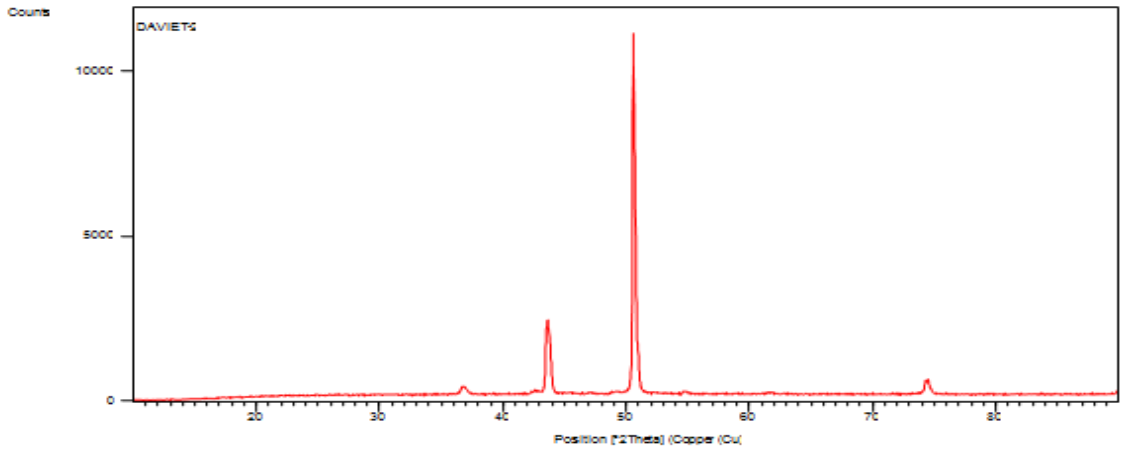

Fig. 7: *XRD Spectrum of Polycrystalline Copper Nanoflowers Synthesized by Electrodeposition.*

Table I: *XRD Spectrum Peaks Data of Polycrystalline Copper Crystals.*

Pos. [°2Th.]	FWHM [°2Th.]	d-spacing [Å]	Rel. Int. [%]	Area [cts*°2Th.]
36.5245	0.2676	2.45814	0.36	49.99
42.4157	0.4015	2.12935	0.12	24.50
43.4459	0.1004	2.08122	3.88	200.54
49.1150	0.2007	1.85343	0.46	47.53
50.4227	0.1020	1.80839	25.07	1779.52
50.5912	0.0816	1.80276	100.00	5678.98
54.7395	0.0816	1.67554	0.66	37.20
74.2673	0.2448	1.27601	0.71	120.45

Table II: *XRD Spectrum Peaks Data of Polycrystalline Copper Nanoflowers.*

Pos. [°2Th.]	FWHM [°2Th.]	d-spacing [Å]	Rel. Int. [%]	Area [cts*°2Th.]
36.7676	0.4684	2.44244	2.34	112.85
42.5816	0.4015	2.12144	0.87	36.16
43.4856	0.0816	2.07941	16.33	185.70
43.6140	0.1020	2.07359	21.49	305.36
43.7749	0.1338	2.06634	14.96	206.40
50.5565	0.1224	1.80392	100.00	1705.38
54.7847	0.3264	1.67427	0.73	33.30
61.6925	0.4896	1.50233	0.38	26.14
74.2904	0.1224	1.27567	3.89	66.27
74.5117	0.1632	1.27243	4.54	103.19

To determine chemical composition and stiochiometry of copper nanorods, FESEM facility was used. EDX spectrum (Figure 8) shows three peaks corresponding to oxygen, copper, and zinc. The quantitative analysis shows chemical composition of nanorods in weight and atom percent (Table III). The zinc impurity of 2.12 atom percent is recorded. It is intriguing that we have encountered the presence of zinc impurity for the first time in copper nanorods.

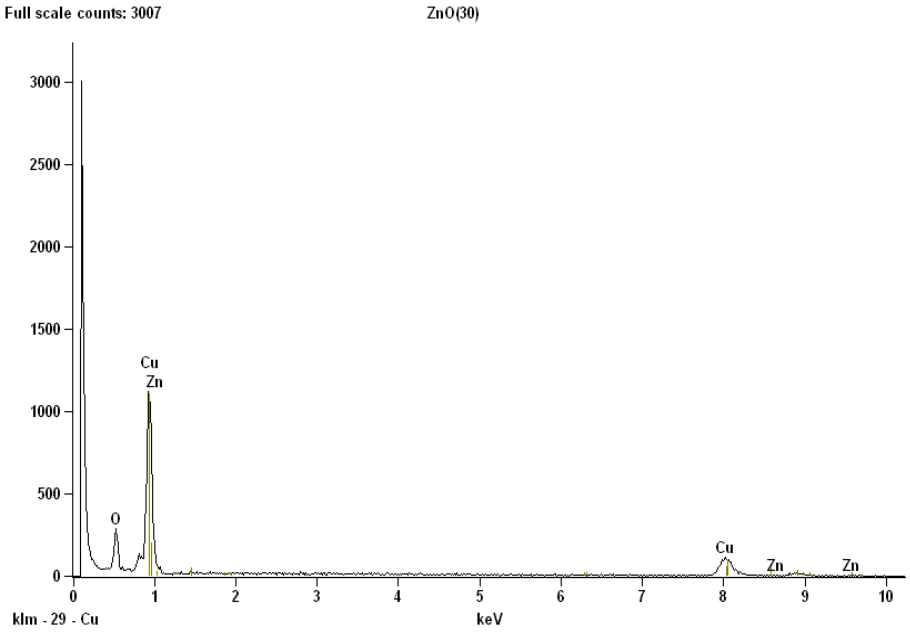

Fig. 8: *EDX Spectrum of Copper Nanorods Showing Peaks of Oxygen, Copper, and Zinc.*

Table III: *Chemical Composition of Copper Nanorods by EDX Analysis.*

Element Line	*Weight %*	*Weight % Error*	*Atom %*	*Atom % Error*
O K	10.02	+/– 0.45	30.69	+/– 1.38
Cu K	87.15	+/–4.56	67.20	+/–3.52
Zn K	2.82	+/– 1.57	2.12	+/–1.18
Total	100.00		100.00	

CTAB-assisted hydrothermal synthesis of CuO nanoflowers is our preliminary investigation. FESEM micrograph (Figure 9) shows the shape of cupric oxide (CuO) nanoflowers. The explanation for CTAB-assisted hydrothermal method of CuO flowers fabrication is given by Zou et al [11]. According to the literature survey, the formation mechanisms of the flower-like CuO nanostructures were different when different preparation methods were used. Yu et al. [16] prepared the flower-like CuO nanostructures by reaction between a Cu plate and a KOH solution at room temperature and

demonstrated their field emission properties. They speculated that the nanoflower was a representative morphology of spherulite formed by radiating growth from a center or a number of centers and the $[Cu\ (OH)_4]^{2-}$ complexes played a key role in the growth of nanoflowers. Zhu et al. [18] obtained the flower-like CuO nanostructures composed of many interconnected needle-like crystallites by hydrolyzing of $Cu(OAc)_2$ solution without any surfactants. Teng et al. [19] synthesized the flower-like CuO nanostructures by hydrothermal process using copper threads as precursor.

They investigated the influences of hydrothermal temperature and hydrothermal time on the nanostructures and reported that the formation of the flower-like structure was controlled not only by the growth thermodynamics, but also by the growth kinetics.

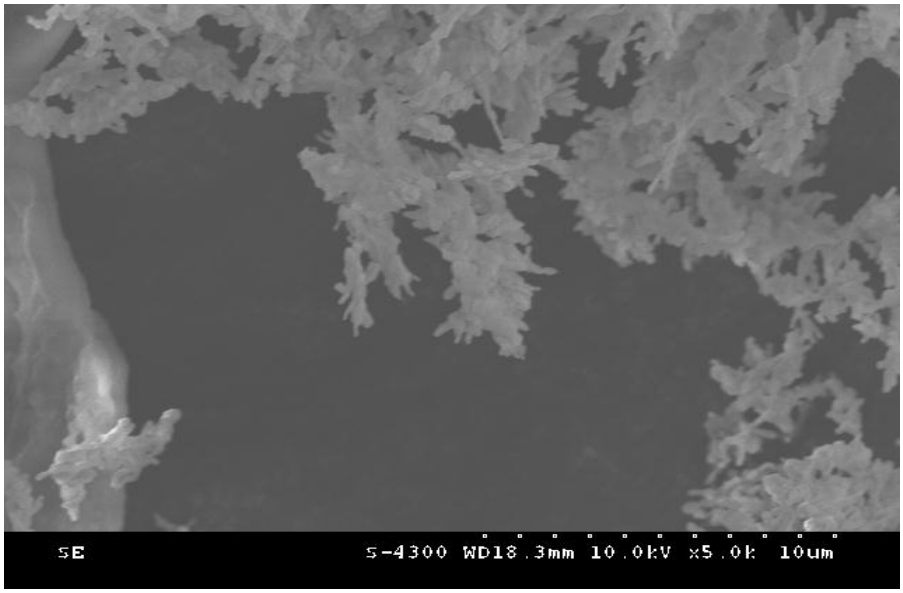

Fig. 9: *FESEM Micrograph of CuO Nanoflowers Prepared by Hydrothermal Method.*

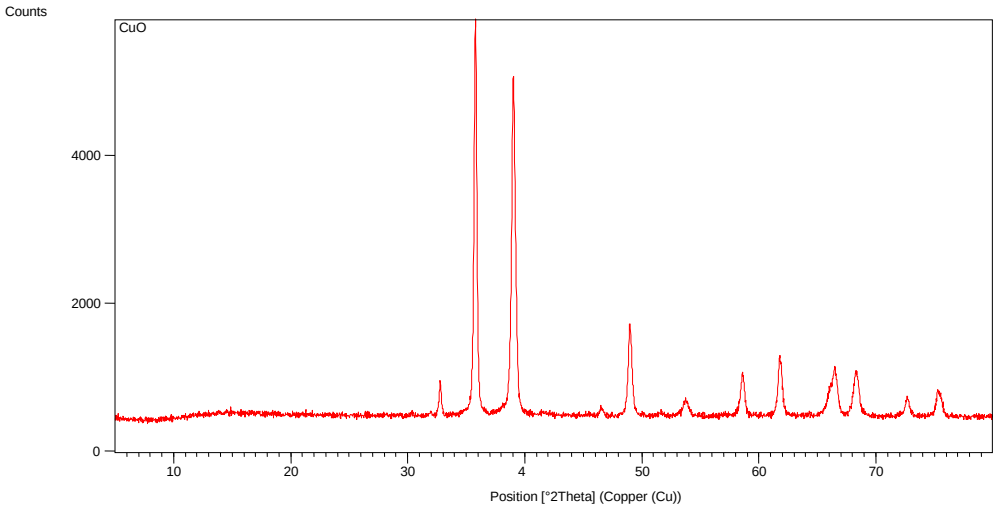

Fig. 10: *XRD Spectrum of Monoclinic Copper Oxide Nanoflowers.*

Table IV: *XRD Spectrum Peaks Data of CuO Nanoflowers.*

Pos. [°2Th.]	FWHM [°2Th.]	d-spacing [Å]	Rel. Int. [%]	Area [cts*°2Th.]
32.7906	0.1338	2.73127	8.01	55.93
35.8066	0.2509	2.50784	100.00	1309.41
38.9983	0.1673	2.30963	83.89	732.34
46.5518	0.2676	1.95095	1.79	24.99
48.9563	0.1506	1.86061	22.75	178.74
53.7459	0.2342	1.70556	4.34	53.09
58.6036	0.3011	1.57524	10.74	168.78
61.7668	0.2007	1.50195	14.27	149.44
66.4776	0.2007	1.40649	12.33	129.17
68.2783	0.1673	1.37372	10.87	94.87
72.6435	0.3011	1.30156	4.59	72.17
75.2766	0.1632	1.26139	6.83	78.61

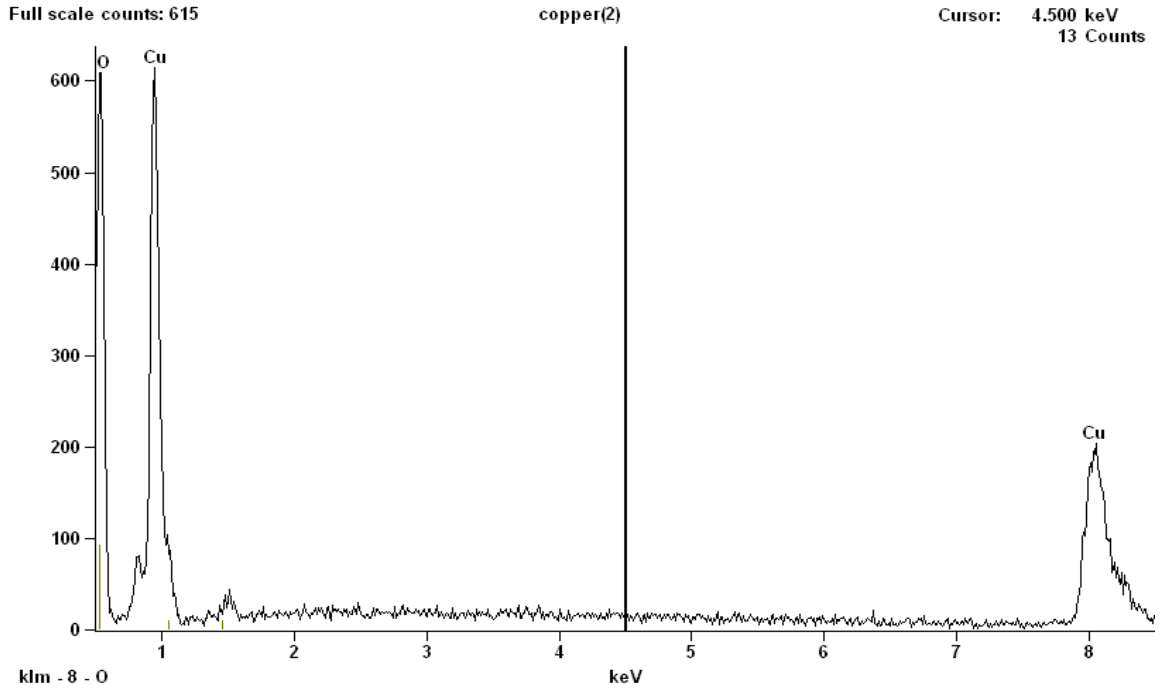

Fig. 11: *EDX Spectrum of Copper Oxide Nanoflowers Prepared by Hydrothermal Method.*

Table V: *Quantitative Results for Copper Oxide Nanoflowers Composition.*

Element Line	Weight %	Weight % Error	Atom %	Atom % Error
O K	33.60	+/– 0.73	66.77	+/– 1.44
Cu K	66.40	+/–3.31	33.23	+/–1.66
Total	100.00		100.00	

The crystallographic structure of copper oxide nanoflowers was investigated by X-ray diffraction analysis (XRD). The typical XRD spectrum (Figure 10) shows 12 peaks (Table IV) with two major peaks at 2θ = 35.8066 and 38.9983, corresponding to Miller indices (111) and (200). All the peaks are compared with the standard XRD spectrum [20] (AMCSD Card Number: 99-101-0934 of American Mineralogist Crystal Structure Database) and a perfect matching exists between the two spectra. In comparison with standard XRD spectrum, the main peak at 2θ = 35.8066 can be indexed to characteristic diffraction of monoclinic phase of CuO with cell parameters (a=0.4653 nm, b= 0.3410 nm, c= 0.5108 nm). The Miller indices of all the peaks in XRD spectrum are represented by (110), (111), (200), (201), (202), (112), (020), (113), (022), (220), (311) and (222). Energy dispersive X-ray analysis (EDX) of CuO nanoflowers was performed using the FESEM facility of Central Scientific Instruments Organization (CSIO), Chandigarh to determine their chemical composition and stoichiometry. The spectrum (Figure 11) reveals three major peaks: two peaks of copper and one peak of oxygen. Table V reveals that the chemical composition of nanoflowers by weight percent and atomic percent are reciprocal. EDX spectrum reveals the chemical purity of CuO nanoflowers as other trace impurities are found to be absent.

4. CONCLUSIONS

Electrodeposition route of template synthesis is an elegant method for fabrication of copper nanoflowers, copper crystals and copper nanorods, using anodic alumina or polymer templates. Over-deposition plays sterling role in the growth of exotic patterns of copper. A variety of copper nanoflowers resembling their counterparts in a botanical garden have been synthesized in our laboratory.

The copper nanoflowers prepared by electrodeposition are polycrystalline in nature with crystallite size of 1.22 nm. The CuO nanoflowers prepared by CTAB-assisted hydrothermal method exhibit monoclinic phase and polycrystalline nature. No scientific theory is yet available to explain their exact nature. It has been discovered that nanoflowers

have great potential for possible applications in nanotechnology. CuO nanoflowers have been exploited as sensor for hydrogen peroxide (H_2O_2) [21] and hydrazine [22], as well as for optical [23] and field emission properties [16].

5. ACKNOWLEDGEMENTS

The author is thankful to the Regional Director and Principal DAVIET, Jalandhar for permission to carry out experiment. Special thanks are due to Dr. Kanchan Sharma and Dr Parveen Kumar of DAVIET for their help in performing this experiment. FESEM analysis was carried out at CSIO, Chandigarh. Author wishes to record his appreciation for Dr Lalit M. Bharadwaj and Dr Inderpreet Kaur for providing research facilities. XRD analysis was carried out at SAIF, Punjab University, Chandigarh and the help of Jagtar Singh is highly appreciated.

REFERENCES

1. Virk. H.S. et al. *J. Nano Res.* 2010.10. 63–67p.
2. Virk. H.S. *J. NanoSci. NanoEngg. & Applications.* 2010. 1(1). 1–14p.
3. Virk. H.S. *Nano Trends.* 2010. 9(1). 1–9p.
4. Virk. H.S. *Int. J. Adv. Engg. & Technol*. 2011. 2(3). 64–68p.
5. Virk. H.S. Chapter 20 of Book *"Nanowires - Implementations and Applications",* Abbass Hashim(Ed.). ISBN: 978-953-307-318-7. InTech Publishers.
6. Virk. H. S. *Pak. J. Chem*. 2011. 1(4). 1–7p.
7. Kharisov. B. I. *Recent Patents on Nanotechnology* 2008. 2(3). 190–200p.
8. Kharissova. O.V. and Kharisov. B.I. *Recent Patents on Nanotechnology.* 2008. 2(2).103–119p.
9. Kharissova. O.V. et al. *Synthesis and Reactivity in Inorganic, Metal-Organic and Nano-Metal Chemistry.* 2009. 39. 662–684p.
10. Kharisov. B.I. and Kharissova. O.V. *Ind. Eng. Chem. Res*. 2010. 49. 11142–11160p.
11. Zou. Y. et al. *Adv. Mater. Res*. 2011. 152–153. 909–914p.
12. Cao. M.H. et al. *Chem. Comm*. 2003. 15. 1884–1885p.
13. Gao. T. et al. *J. Physics: Condensed Matter*. 2002. 14. 355–363p.
14. Kumar. S. et al. *Superlattices and Microstructures.* 2008. 43. 324–329p.
15. Erdey-Gruz. T. and Volmer. M. *Z. Phys. Chem*. 1930. 150A. 203–213p.
16. Yu. L.G. et al. *J. Cryst. Growth*. 2008. 310. 3125–3130p.
17. Cullity. D.B. *Elements of X-ray Diffraction* (Addison-Wesley Inc. Massachusetts, USA1956).
18. Zhu. J.W. et al. *Mater. Lett*. 2007. 61. 5236 –5238p.
19. Teng. F. et al. *Sensors & Actuators B.* 2008. 134. 761–768p.

20. Downs. R.T. and Hall-Wallace. M. *American Mineralogist*. 2003. 88. 247–250p.
21. Gu. A. et al. *Bull. Material Sci*. 2010. 33(1). 17–20p.
22. Zhang. X. et al. *Chem. Letters.* 2009. 38(5). 466–467p.
23. Luo. Y. et al. *Dianzi Yuanjian Yu Cailiao* (Chinese). 2007. 26(2). 11–13p.

